Serial No. N7616 **NAFO SCR Doc. 25/001**

SCIENTIFIC COUNCIL MEETING – JANUARY 2025

Dynamic Factor Analysis for 3LN redfish survey indices

Perreault A.[1], Hatefi F.[1]

[1]Northwest Atlantic Fisheries Centre
Fisheries and Oceans Canada, 80 East White Hills Road
St. John's, Newfoundland and Labrador, A1C 5X1, Canada

PERREAULT, A., & HATEFI, F. 2025. Dynamic Factor Analysis for 3LN redfish survey indices. Scientific Council Research Document, SCR Doc. 25/001: 1-16.

Introduction

Dynamic factor analysis (DFA) is a dimension-reduction technique used to model multiple time series in terms of a smaller number of latent states (i.e., common trends; Zuur et at., 2003). The main objectives of this DFA analysis are to:

1) Identify if common trends exist in the 3LN redfish survey time series
2) Identify if there are relationships between these trends and ocean climate, ecosystem and/or exploitation indicators, and
3) Assess if the results can be integrated into a pre-existing model (ACL/SURBA) to help explain/reduce process variance.

Methods

Data inputs

The data used for the analyses are abundance at length estimates from the Canadian 3LN fall (1995-2021) and spring (1995-2021) RV survey series and the 3N and 3L EU-Spain RV series (2003-2022). Length-aggregated adult indices were derived from lengths greater than 14cm and length-aggregated juvenile indices from those greater than 9 and less than 15 cm (Fig. 1). The juvenile lengths were chosen for consistency with the most recent stock assessment (Perreault et al., 2024).

Additional data series for twelve external factors, including nine related to ocean climate, one relating to exploitation and two relating to ecosystem drivers were compiled for the 3LNO area (Figs 2-5, Table 1; Cyr et al., 2024, Cyr & Bélanger, 2024, Perreault et al., 2024). Where the data allowed, the covariates were lagged up to ten years (Table 1). All timeseries were normalized prior to inclusion in the models.

Model fit and selection

The DFA model is detailed in Appendix A, however in simple terms, the model can be described as

data=common trends + noise, **H**,

where **H** is the covariance matrix for the observation error. The number of common trends was allowed to vary between 1 and 3, based on initial model explorations. External covariates were included as

data=common trends + explanatory variable + noise, **H**.

A suite of DFA models were fit using the MARSS package in R (Holmes et al., 2024) and combinations of number of trends (1-3), covariates (Table 1) and **H** structure (diagonal and equal, diagonal and unequal or unconstrained). Additionally, models with up to four covariates were fit.

The best fitting model was selected via AICc, inspection of residual plots and overall fit. Additional sensitivity runs were also explored and included:

1) Fitting separate models for the juvenile and adult series and,

2) Fitting the model to data from 1991-2022 and from 2000-2022 to determine if relationships between covariates break down given time series length

Results

Preliminary model fits found that the 3L EU-Spain index was relatively noisy and the models wanted to attribute most of the variability to this series. Since the 3L EU-Spain index covers the shortest time period and a small portion of the survey area, it was subsequently dropped from the analysis.

Overall, models with two latent states (or common trends) and **H** diagonal and equal performed best. When including only one covariate, models that included bottom spring and fall temperatures, landings, and sea surface temperature had lower AICcs than the model with no covariates.

The best fitting DFA model had two common trends and bottom spring temperatures (lagged three years) and the cold intermediate layer (CIL; lagged ten years) as covariates. The significance of the ocean climate drivers varied by survey, with the spring bottom temperatures strongly related to the 3N EU-Spain juvenile and adult indices and the CIL strongly related to the fall adult and 3N EU-Spain juvenile indices. The first common trend had significant factor loadings for all adult indices (fall, spring, EU-Spain) while the second common trend had significant loadings for all juvenile indices (Figs 6-7). Although there were some similarities in the two common trends, the juvenile trend tended to decrease in periods of high adult trend (Fig 8).

Model fits to the data were generally good, with little to no patterns seen in the residual plots (Figs 9-11). Additionally, sensitivity runs that truncated or elongated the time series identified similar covariates as the full model. The model with data from 2000-2022 had two common trends and CIL(10) as a covariate for the best fitting model (Figs 12-13), while the model with data from 1991-2022 had two common trends and landings(4) and bottom spring temperatures(9) as covariates for the best fitting model (Figs 14-15).

When DFA models were fit separately to the adult and juvenile series, the results were somewhat different, with the adult model identifying one common trend and bottom spring temperatures (3), CIL(10) and landings(4) as covariates for the best fitting model. The DFA models fit to the juvenile series identified two common trends and the Newfoundland climate index (2) as the best fitting model.

Discussion

Our final DFA model identified two common trends, one that described 3LN redfish adult survey indices (adult common trend) and one that described juvenile indices (juvenile common trend), that were related to a combination of lagged ocean climate drivers (cold intermediate layer, lagged ten years; spring bottom temperatures, lagged three years). However, the significance of the ocean climate drivers varied by survey, with the spring bottom temperatures strongly related to the 3N EU-Spain juvenile and adult indices and the cold intermediate layer strongly related to the fall adult and 3N EU-Spain juvenile indices.

The juvenile common trend tended to decrease following high levels of adult common trend, providing some evidence of density dependence for the 3LN redfish stock. This is not entirely unexpected as similar evidence for density-dependent population controls has been found for redfish in other regions (e.g., Bown-Vuillemin et al., 2022; Marquez et al., 2023).

Sensitivity runs that truncated or elongated the time series identified different subsets of external drivers than our final model, with the elongated time series identifying commercial landings and bottom spring temperatures as the main drivers and the truncated series identifying the CIL alone. Redfish are slow-growing and long-lived and the time scale over which the stock reacts to external drivers may span decades; therefore, the truncated model may not capture the influence of external drivers for such a short period. Additionally, the longer time series covers the era where the stock was heavily fished, which helps explain the significance of the commercial landings in the model that includes more data. In all cases, no matter the time period selected, the dynamics of redfish appear to be partially explained by ocean climate drivers, and these are an important source of variability that is currently ignored in the stock assessment.

Our DFA model found that the spring bottom temperatures were strongly related to the 3N EU-Spain juvenile and adult indices but were not significant for the fall and spring indices. The EU-Spain and the Canadian spring surveys both occur in May-June, therefore similarities in ocean climate drivers across surveys were expected. However, the Canadian spring survey covers the full 3LN survey area, the 3N EU-Spain survey covers the portion of 3N outside the 200nm zone, and the spring bottom temperature index is aggregated across the full 3LNO area. Bottom temperatures in 3NO are the highest in the Grand Bank region, mainly driven by the presence of the Labrador Slope water and atmospheric forcing along the slope of the bank (Cyr et al., 2024). Therefore, the spring bottom temperature used in the model may better capture the variability in the environment for the 3N EU-Spain stock. Future DFA models that integrate ocean climate factors at a finer resolution (e.g. bottom temperature by depth; Coyne et al., 2025) may provide more insight and consistency on drivers of 3LN redfish dynamics.

The Grand Bank of Newfoundland is a highly dynamic region, influenced by the warm waters of the Gulf Stream and the cooler waters of the Labrador current, and it is therefore not unexpected that our DFA models identified ocean climate drivers as having a strong influence on redfish juvenile and adult dynamics. A stock assessment model that integrates ocean climate drivers may provide a better fit to the data and help explain large process error variances estimated in the current model (Perreault & Hatefi, 2024). However, how to integrate these into the model remains difficult given a lack of understanding of the mechanisms driving these processes.

Figures

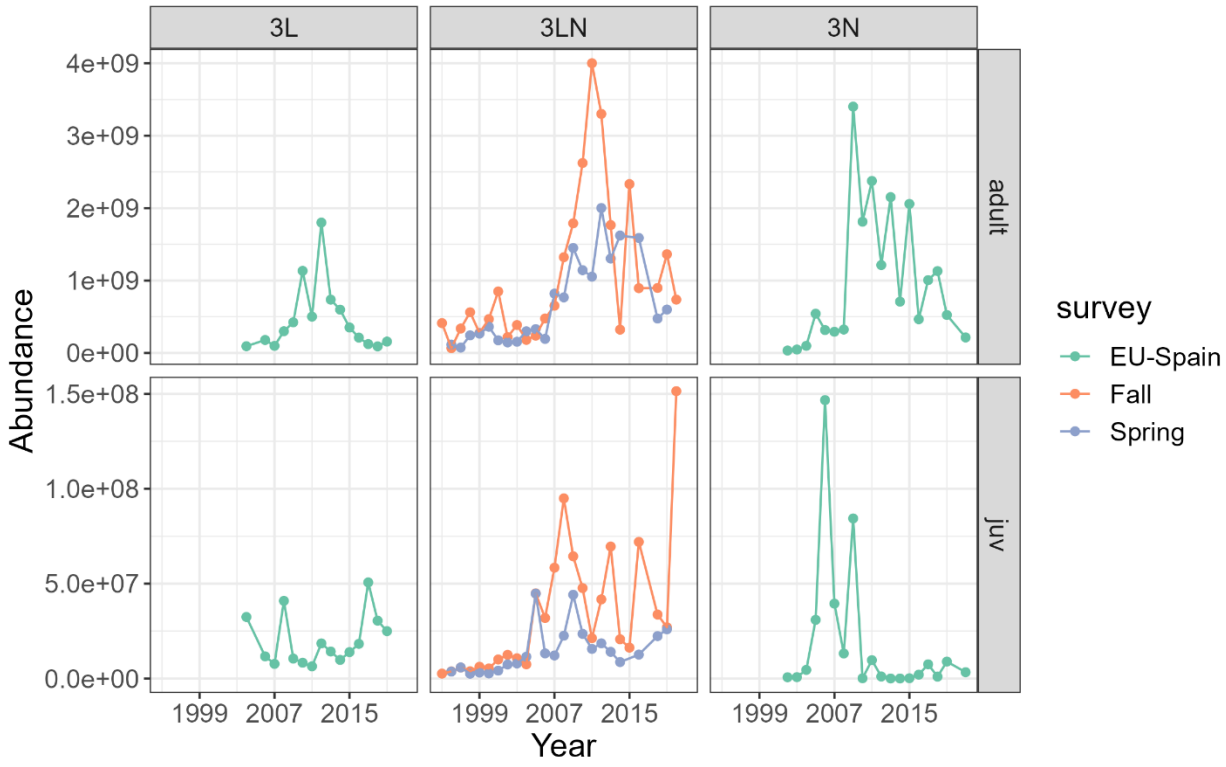

Figure 1. Data inputs considered for the DFA model (3LN Fall, Spring and 3N EU-Spain used in the final models)

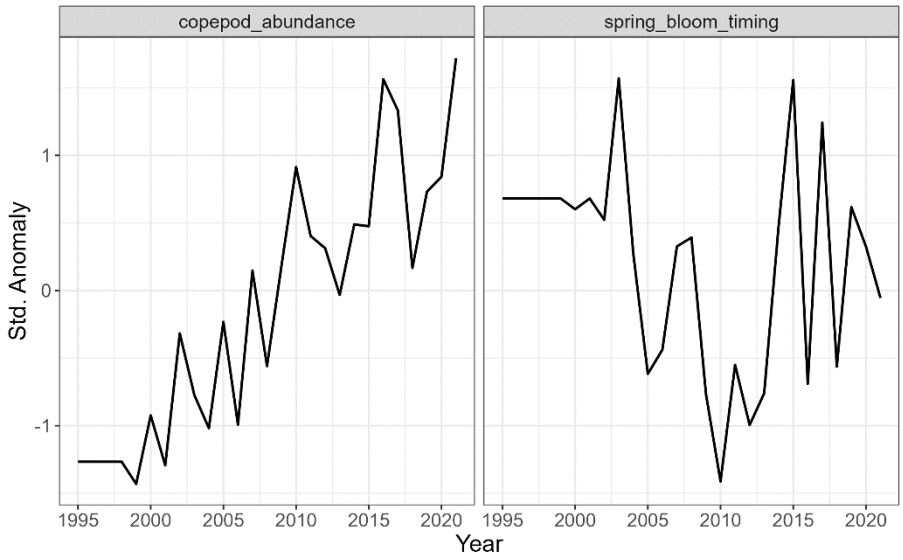

Figure 2. Ecosystem external factors considered in the DFA models

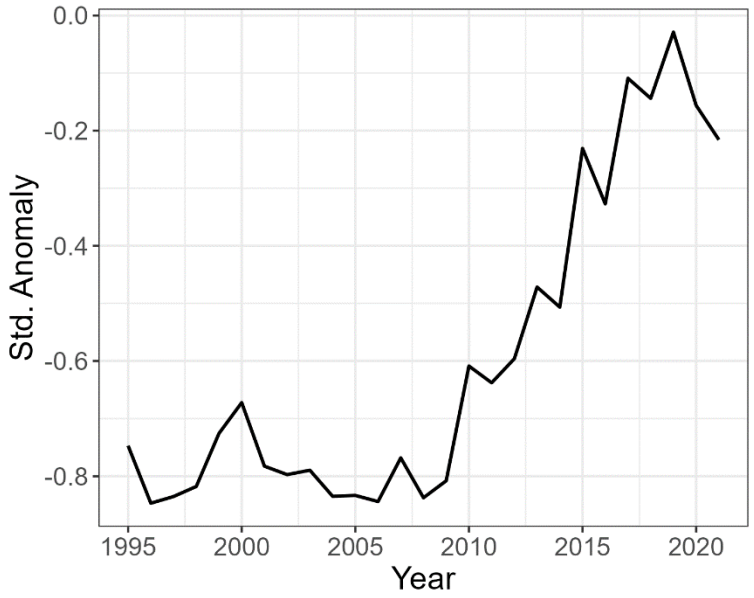

Figure 3. Exploitation (3LN redfish commercial landings) external factors considered in the DFA models

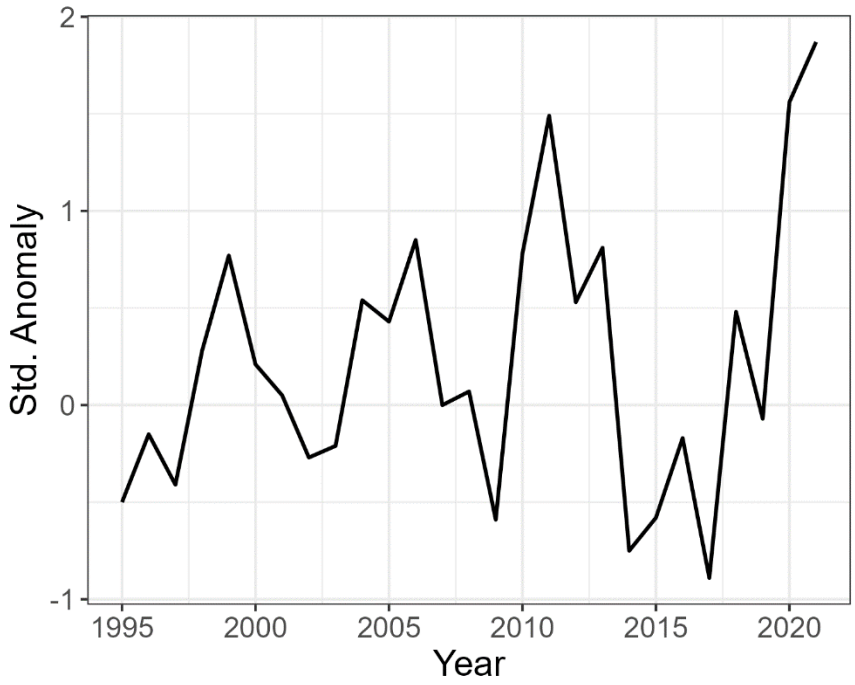

Figure 4. Ocean climate external factor (3LNO NL ocean climate index) considered in the DFA models

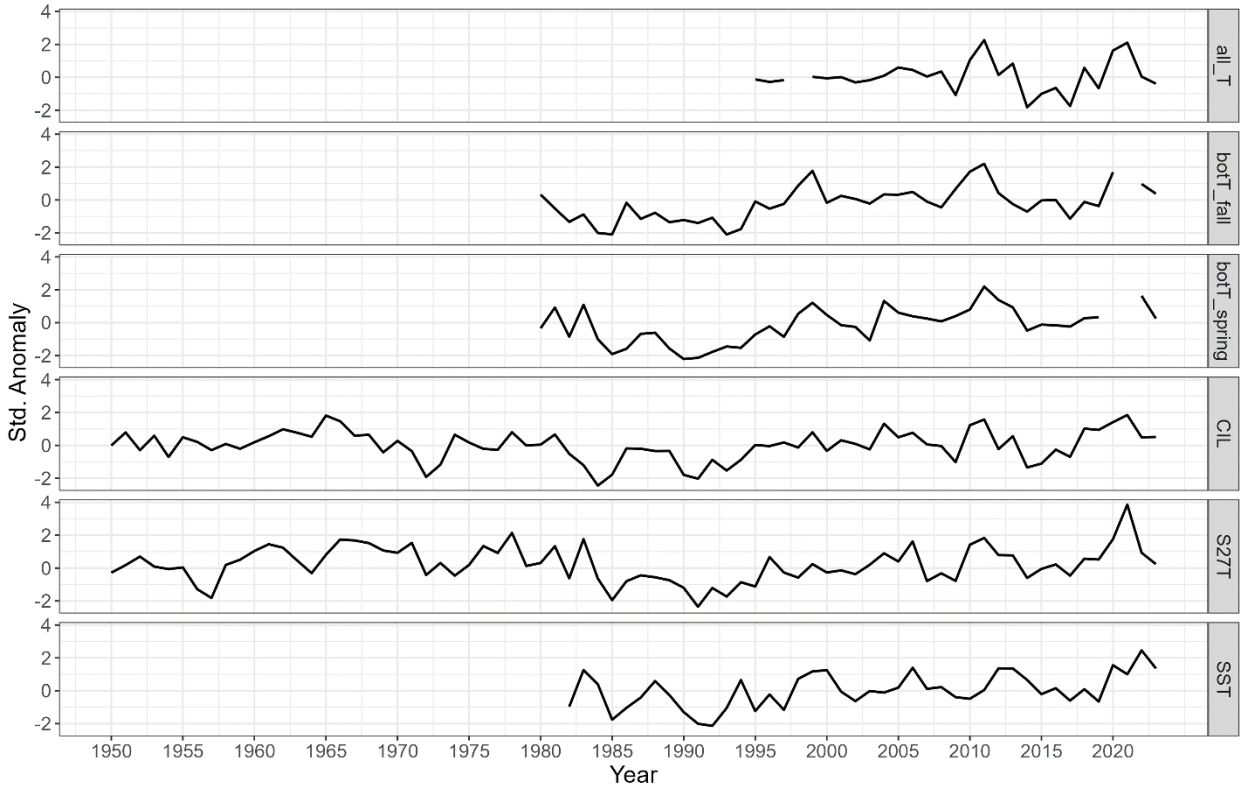

Figure 5. Disaggregated 3LNO Newfoundland climate index (see Table 1 for definitions of indices) considered as external factors in the DFA models

Figure 6. DFA model estimated common trends with 95% confidence intervals

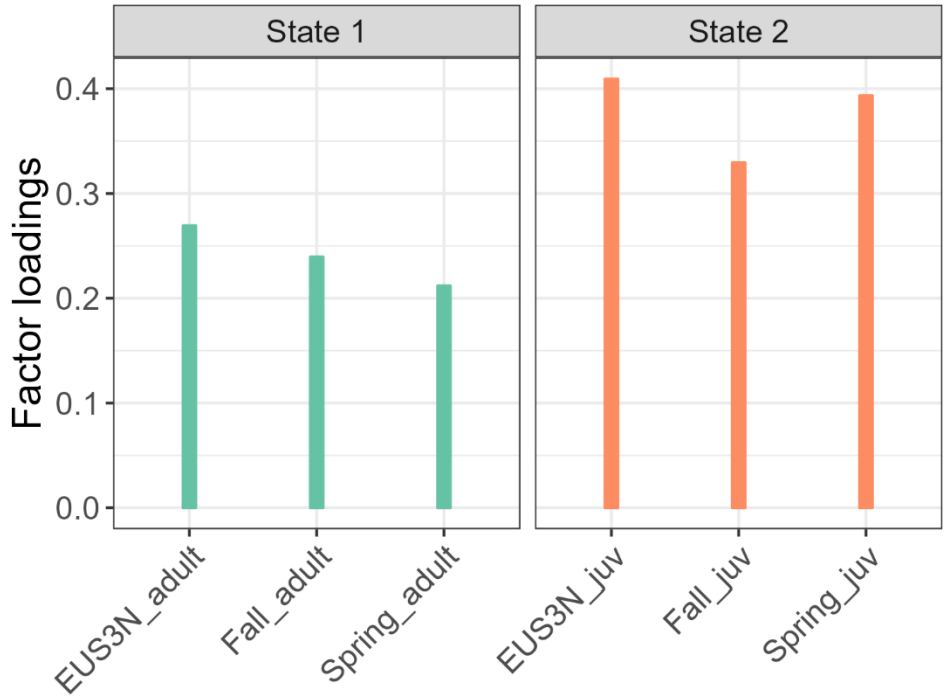

Figure 7. DFA model predicted factor loadings (loadings > |0.2| strongly significant)

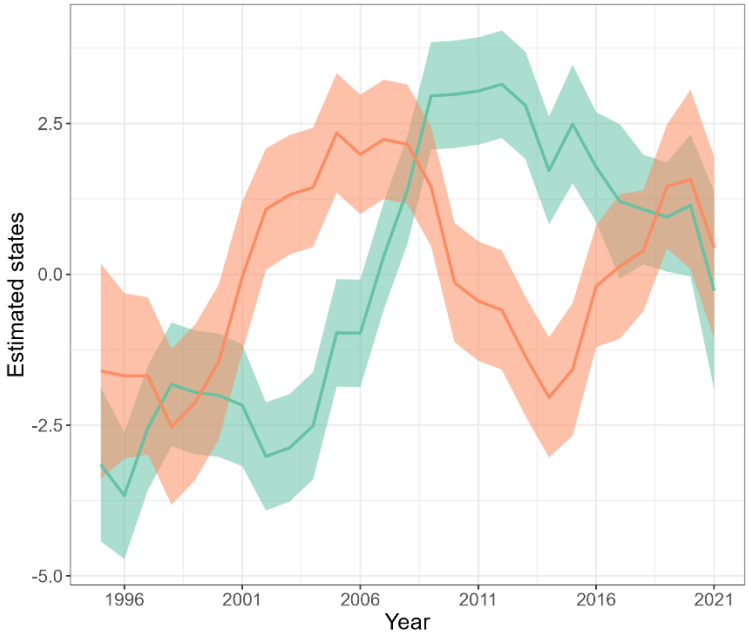

Figure 8. DFA model estimated common trends with 95% confidence intervals

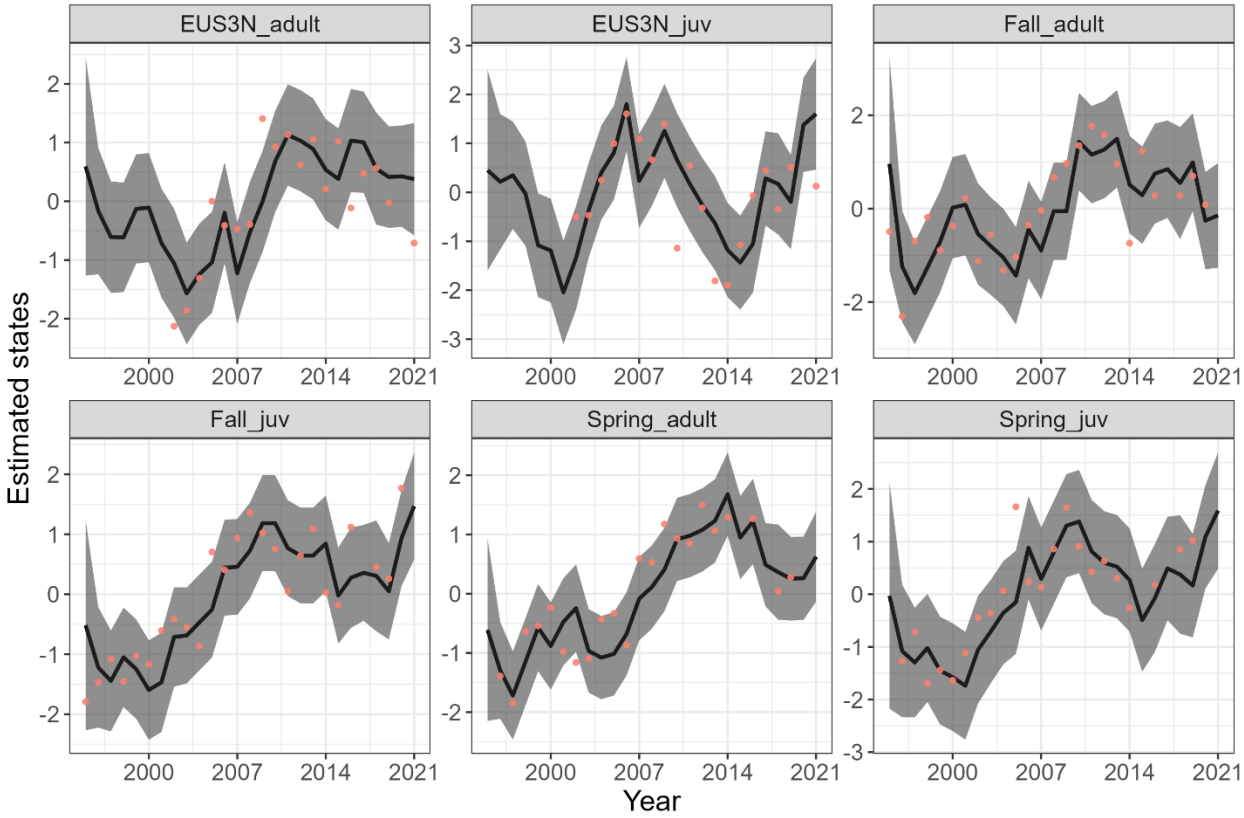

Figure 9. DFA model observed (red) vs predicted (grey) indices

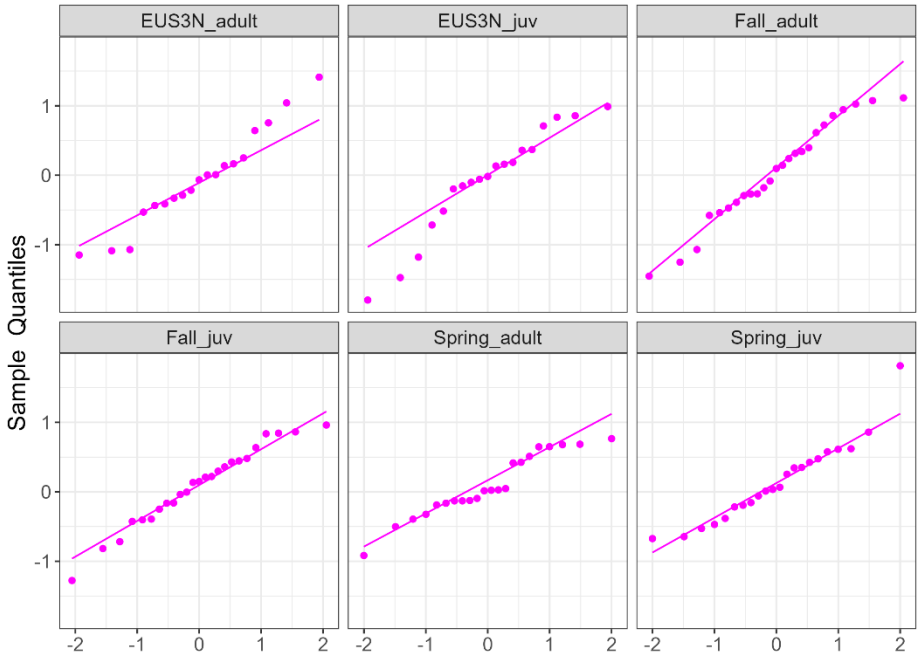

Figure 10. DFA model standardized residual quantile-quantile plots

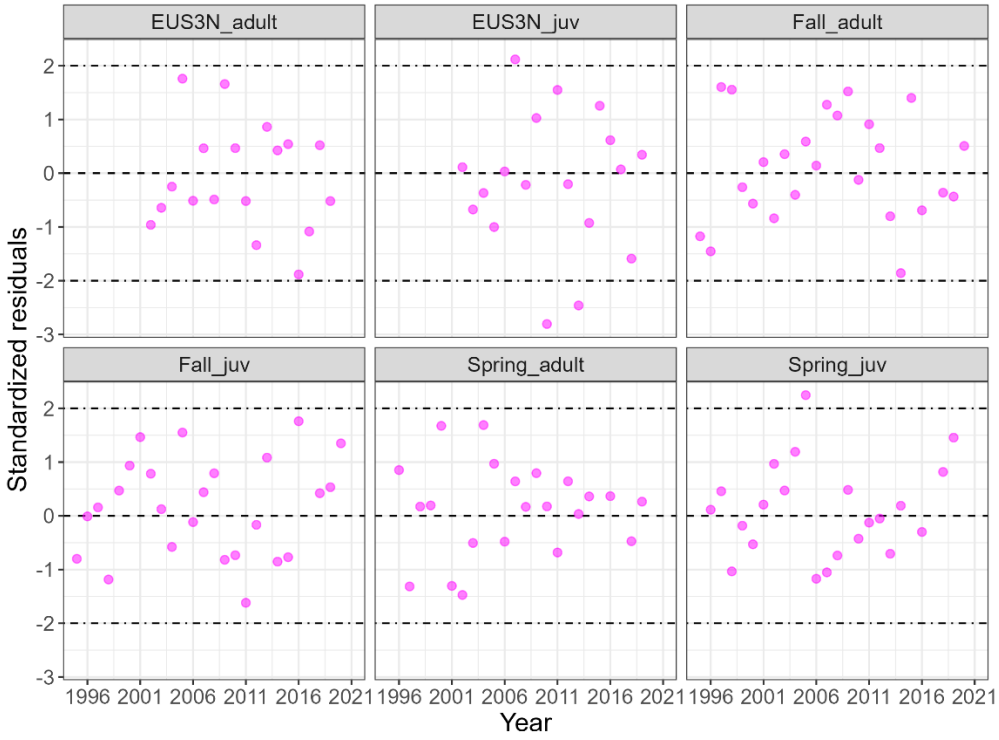

Figure 11. DFA model standardized residual vs year plots

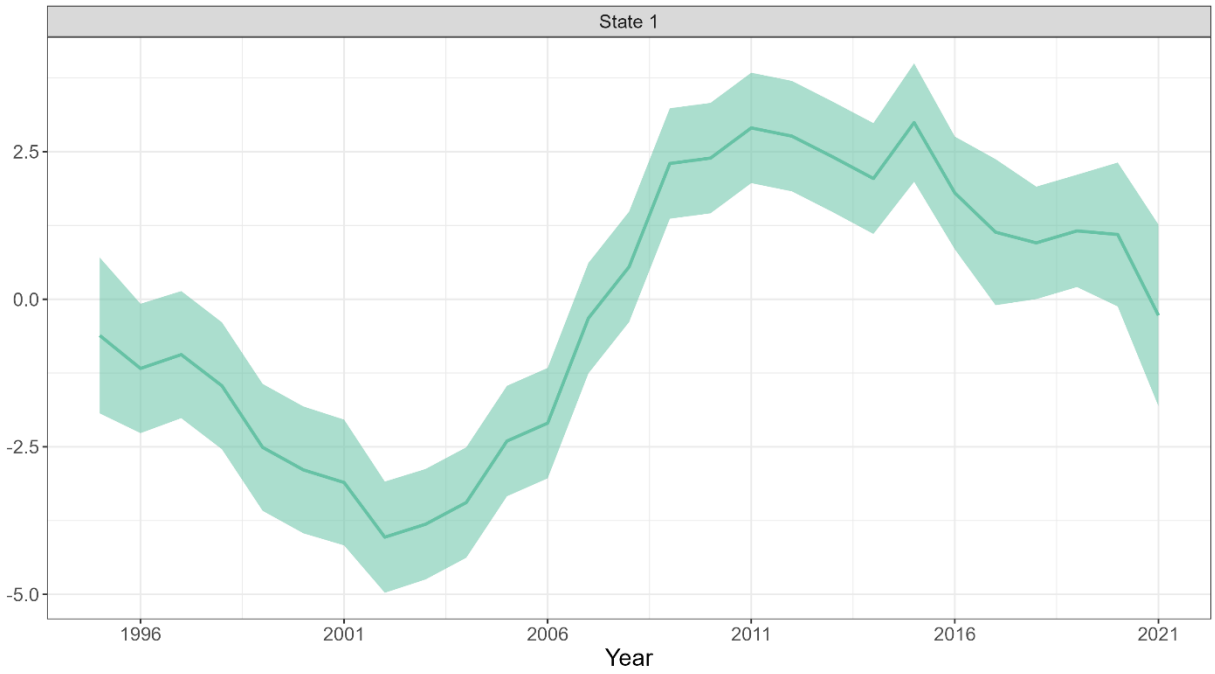

Figure 12. DFA adult model estimated common trends with 95% confidence intervals

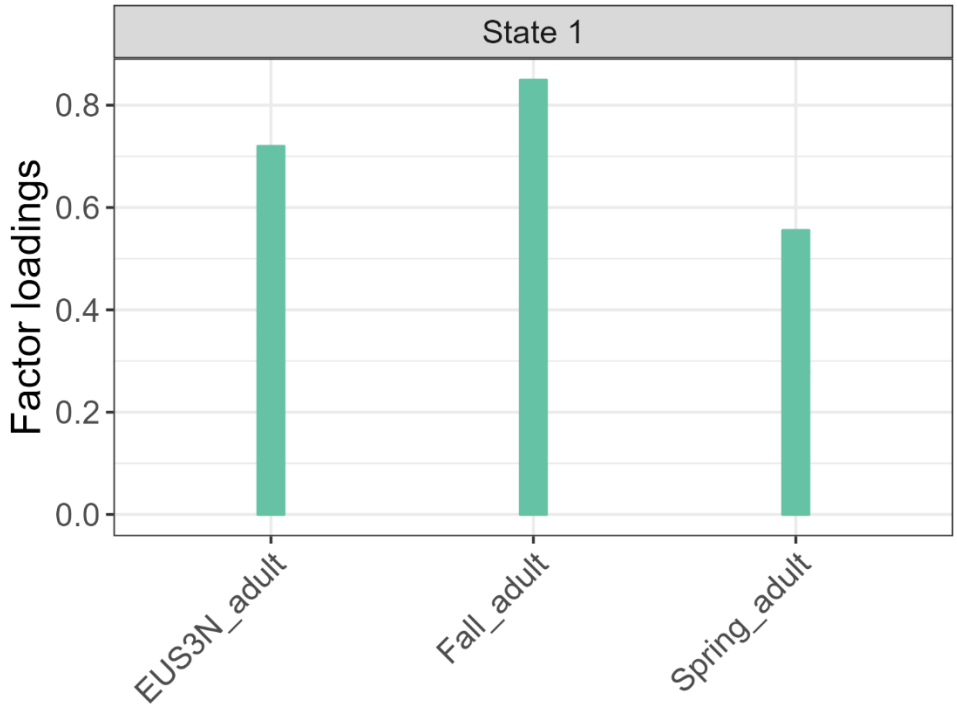

Figure 13. DFA adult model predicted factor loadings (loadings > |0.2| strongly significant)

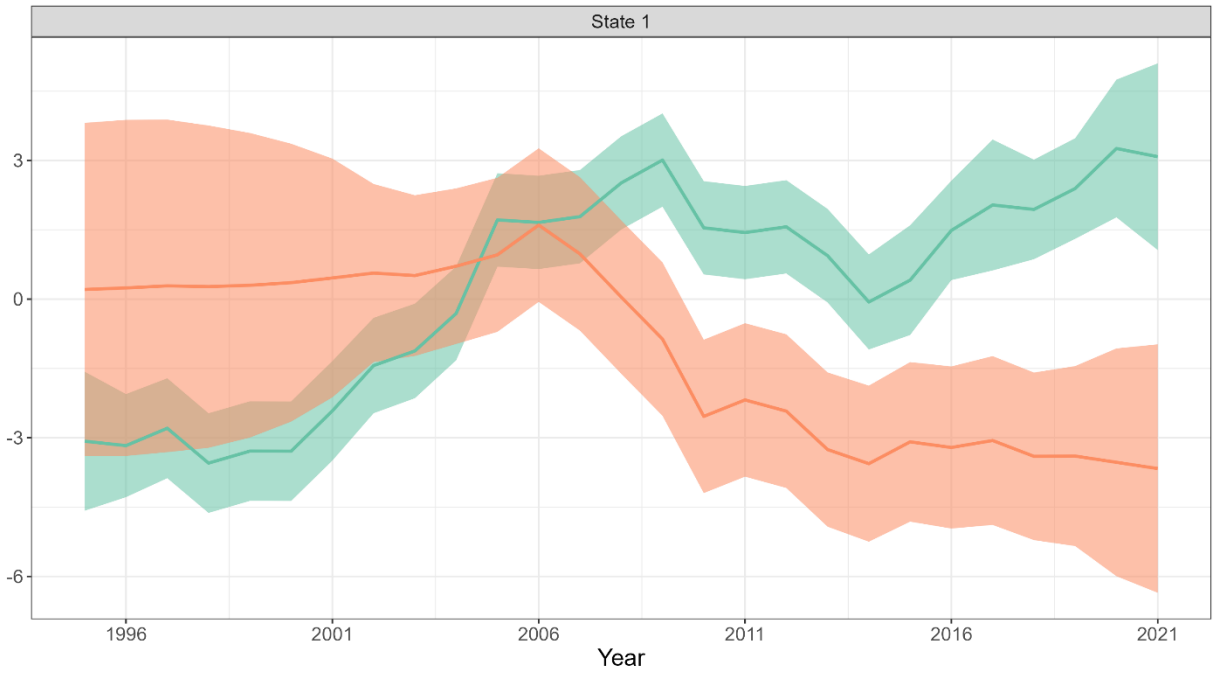

Figure 14. DFA juvenile model estimated common trends with 95% confidence intervals

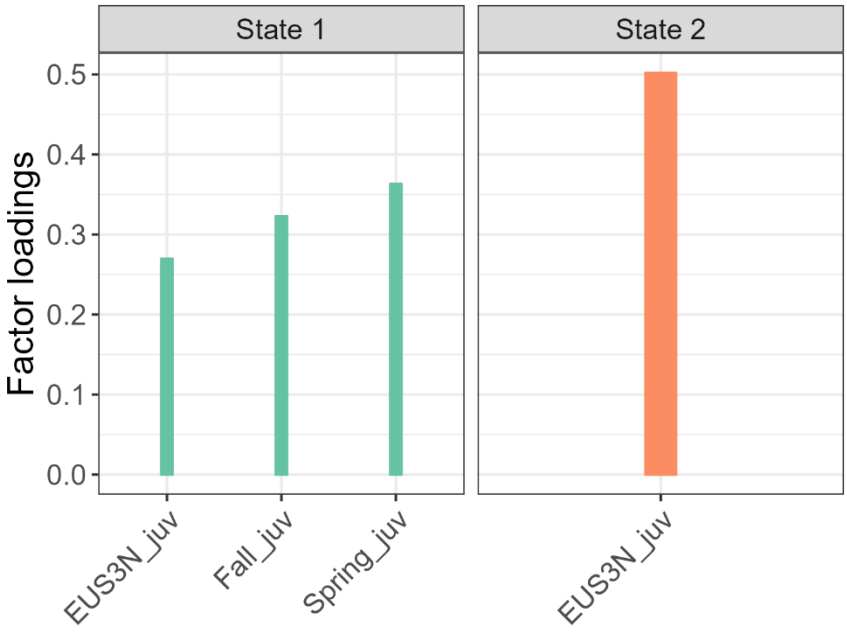

Figure 15. DFA juvenile model predicted factor loadings (loadings > |0.2| strongly significant)

Tables

Table 1. Data inputs and covariates used in the DFA model. all_T = Seal Island (SI), Bonavista (BB), Flemish Cap (FC) section mean temperature, botT_fall = 3LNO fall bottom temperature, botT_spring = 3LN spring bottom temperature, CIL = SI, BB, FC Cold Intermediate Layer area, S27_T = mean temperature at Station 27, SST = 3LNO mean surface temperature, botT_index_fall = mean 3LN fall RV bottom temperatures for redfish index strata, botT_index_spring = mean 3LN spring RV bottom temperatures for redfish index strata

		Justification	Reference
Inputs	3LN fall adult/juvenile 3LN spring adult/juvenile 3N EU-Spain adult/juvenile	-	-
Covariates (lag)			
Ocean climate	3LNO ocean climate index (10)	Good indicator of overall ocean climate	Cyr et al., 2024
	Disaggregated 3LNO ocean climate index: S27T (10), CIL(10); SST(10); all_T(10) botT_fall (10); botT_spring (10)	Aggregated ocean climate index may mask underlying relationships	
	botT_index_fall (10); botT_index_spring (10)	Redfish are known to be depth preferential; bottom temperature in redfish index strata may differ from the full 3LNO fall and spring bottom temperatures	Perreault et al., 2023
Ecosystem	Copepod abundance (0) Spring bloom timing (0)	Available diet composition research suggests that *Calanus finmarchicus* is a primary larval food source in the Gulf. Timing of bloom positively correlated with recruitment in the Gulf	Burn et al., 2020 Roberts et al., 2024
Exploitation	Commercial landings (10)		

Table 2 DFA model parameter estimates and standard errors. F1 and F2 are factor loadings for State 1 and State 2, respectively.

term	estimate	std.error
F1Fall_adult	0.476	0.103
F1Fall_juv	0.223	0.103
F1Spring_adult	0.32	0.078
F1Spring_juv	0.247	0.128
F1EUS3N_adult	0.362	0.1
F1EUS3N_juv	-0.002	0.142
F2Fall_juv	0.289	0.078
F2Spring_adult	-0.022	0.054
F2Spring_juv	0.373	0.097
F2EUS3N_adult	-0.138	0.074
F2EUS3N_juv	0.427	0.107
R.diag	0.171	0.026
D.(Fall_adult,BOT_S)	-0.077	0.165
D.(Fall_juv,BOT_S)	0.065	0.141
D.(Spring_adult,BOT_S)	0.262	0.139
D.(Spring_juv,BOT_S)	-0.15	0.163
D.(EUS3N_adult,BOT_S)	-0.4	0.163
D.(EUS3N_juv,BOT_S)	-0.57	0.172
D.(Fall_adult,CIL)	-0.469	0.157
D.(Fall_juv,CIL)	0.225	0.138
D.(Spring_adult,CIL)	0.058	0.145
D.(Spring_juv,CIL)	0.188	0.17
D.(EUS3N_adult,CIL)	0.109	0.18
D.(EUS3N_juv,CIL)	0.385	0.19

Table 3 Summary of significant factor loadings (greater than |0.2|) and ocean climate variables (*t*-values>2)

	Trend1	Trend2	SpringBT(3)	CIL(10)
Fall_adult				-0.47
Fall_juv				
Spring_adult				
Spring_juv				
EUS3N_adult			-0.40	
EUS3N_juv			-0.57	0.38

Appendix A: DFA Model

The DFA model is described by two equations, namely the state process (Eq. 1) and the observation process (Eq. 2), where x_t is a vector of *m* latent states (common trends) at time *t,*

$$x_t = x_{t-1} + \partial_t \qquad \partial_t \sim MVN(0, \boldsymbol{Q}) \tag{1}$$

with process noise ∂_t and covariance matrix $\boldsymbol{Q}$.

The observed time series (y_t) are modeled as a linear combination of the latent states and observation covariates,

$$y_t = \boldsymbol{\Gamma} x_t + D_t d_t + \varepsilon_t \qquad \varepsilon_t \sim MVN(0, \boldsymbol{H}) \tag{2}$$

where $\boldsymbol{\Gamma}$ are the factor loadings linking the latent states to the observed series, d_t are the observation covariates and D_t are the fixed parameters estimating the influence of d_t on the observations. The observation noise is ε_t with covariance matrix $\boldsymbol{H}$.

Simplifying assumptions are required for the model to be identifiable, namely $\boldsymbol{Q}$ is set to the identity matrix and the first m−1 rows of Γ set to 0 if *j* > *i* for the *j*-th column and *i*-th row.

The covariance matrix $\boldsymbol{H}$ can take on a variety of forms, however for our application we explored

1) diagonal and equal – all non-diagonal elements of $\boldsymbol{H}$ = 0 and equal otherwise (i.e. one variance parameter shared across surveys),

2) diagonal and unequal – all non-diagonal elements of $\boldsymbol{H}$ = 0 and free otherwise (i.e. separate variance parameter for each survey but independent), and

3) unconstrained – diagonal and off diagonal elements of **H** freely estimated (i.e. separate variance and covariance across surveys).

References

Brown-Vuillemin, S., Chabot, D., Nozères, C., Tremblay, R., Sirois, P., & Robert, D. (2022). Diet composition of redfish (Sebastes sp.) during periods of population collapse and massive resurgence in the Gulf of St. Lawrence. *Frontiers in Marine Science*, *9*, 963039.

Coyne, J., Cyr, F., Donnet, S., Galbraith, P., Geoffroy, M., Hebert, D., ... & Walkusz, W. (2025). Canadian Atlantic Shelf temperature-salinity (CASTS).

Cyr, F., Coyne, J., Galbraith, P. S., Layton, C., & Hebert, D. (2024). Environmental and Physical Oceanographic Conditions on the Eastern Canadian shelves (NAFO Sub-areas 2, 3 and 4) during 2023. In NAFO Scientific Council Meeting Scientific Council Report, SCR Doc (Vol. 24, No. 010).

Cyr, F., & Bélanger, D. (2024). Environmental indices for NAFO subareas 0 to 4 in support of the Standing Committee on Fisheries Science (STACFIS) – 2023 update. In NAFO Scientific Council Meeting Scientific Council Report, SCR Doc (Vol. 24, No. 012).

Holmes EE, Ward EJ, Scheuerell MD, Wills K (2024). MARSS: Multivariate Autoregressive State-Space Modeling. R package version 3.11.9, https://CRAN.R-project.org/package=MARSS.

Marquez, J. F., Herfindal, I., Sæther, B. E., Aanes, S., Salthaug, A., & Lee, A. M. (2023). Effects of local density dependence and temperature on the spatial synchrony of marine fish populations. Journal of Animal Ecology, 92(11), 2214-2227.

Perreault, A., Wheeland, L., Regular, P., Koen-Alonso, M. & Rideout, R. An Assessment of the Status of Redfish in NAFO Divisions 3LN. In NAFO Scientific Council Meeting Scientific Council Report, SCR Doc (Vol. 24, No. 048).

Perreault, A., Rogers, B., & Varkey D. Wheeland, L., Regular, P., Koen-Alonso, M. & Rideout, R. Data selection for 3LN redfish in preparation for an updated management strategy evaluation. In NAFO Scientific Council Meeting Scientific Council Report, SCR Doc (Vol. 23, No. 001).

Zuur, A. F., Tuck, I. D., & Bailey, N. (2003). Dynamic factor analysis to estimate common trends in fisheries time series. Canadian journal of fisheries and aquatic sciences, 60(5), 542-552.